Low-energy paramagnetic spin fluctuations in the weak itinerant ferromagnet MnSi

Y. Ishikawa

Physics Department, Tohoku University, Sendai, 980 Japan

Y. Noda

Sendai Radio Technical College, Miyagi, 989-31 Japan

C. Fincher and G. Shirane

Brookhaven National Laboratory, Upton, New York 11973

(Received 27 July 1981)

Low-energy paramagnetic excitations in the weak itinerant ferromagnet (WIF) MnSi have been studied by neutron scattering. The observed spectrum has a Lorentzian form $(\Gamma/\Gamma^2+\omega^2)$ and is clearly separated from excitations in the Stoner continuum. The generalized susceptibility, $\mathcal{X}(q)$, has been obtained by integrating the scattering intensity over energy. It is found that $\mathcal{X}(q)$ depends upon the wave vector q as $\mathcal{X}(q)^{-1}=\kappa^2(T)+q^2$ for $q \leq 0.125(2\pi/a)$ with $\kappa^2(T)=\kappa_0^2(T-T_c)$. After extrapolating these results to $q=0$, it is found that $\mathcal{X}(q=0)$ follows the Curie-Weiss law, suggesting that the observed spin fluctuations correspond to the Moriya-Kawabata (MK) spin fluctuations responsible for the Curie-Weiss dependence of the static susceptibility of a WIF. The linewidth Γ is found to be proportional to $q/\mathcal{X}(q)$ as predicted by the MK theory, in contrast with the $q^2/\mathcal{X}(q)$ relation expected in a Heisenberg system. These results provide the first direct experimental evidence for the existence of MK spin fluctuations in a WIF above T_c.

I. INTRODUCTION

The cubic intermetallic compound MnSi is a *typical* itinerant helimagnet with a long period of 180 Å.[1] It is magnetically saturated in a relatively weak field of 6 kOe and exhibits the typical characteristics of a weak itinerant ferromagnet.[2] Neutron scattering has detected the well-defined spin-wave excitations below 2.5 meV and the broad excitations in the Stoner continuum above 2.5 meV as described in a previous paper[3] (referred to as I hereafter). The spin-wave dispersions renormalize with increasing temperature, but the excitations in the Stoner continuum remain unchanged even at temperatures ten times higher than the Néel temperature $T_N=29.5$ K. The general features of the spin dynamics are qualitatively in good agreement with what is expected for a weak itinerant ferromagnet based on the random-phase approximation (RPA)-type band theory.

The simple band theory is, however, found inappropriate for describing the magnetic properties above the Néel temperature. The static susceptibility $\mathcal{X}(0)$ obeys the Curie-Weiss law with the effective moment of $1.4\mu_B$, which is much higher than the saturation moment of $0.4\mu_B$ at the lowest temperature.[4] The nuclear-spin relaxation time T_1 in the paramagnetic region is independent of temperature as is the case with a localized spin system, but has a value 2 orders of magnitude smaller than the case where the localized spin $1.4\mu_B$ exists.[5] Recent polarized neutron scattering also suggests the existence of fairly large magnetic moments of order of $2\mu_B$ in MnSi in the paramagnetic region, which seemingly increase with increasing temperature.[6] In order to reconcile these inconsistent *thermodynamical* properties, Moriya and his collaborators have developed the spin-fluctuation theory for itinerant magnetic materials where the spin fluctuations are taken into account in the self-consistent ways [the self-consistent renormalization (SCR) theory].[7-9] In the weak itinerant ferromagnet, the SCR theory, often referred to as the Moriya-Kawabata (MK) theory, predicts low-energy spin fluctuations (the MK fluctuations) in the small q regions which contribute to produce

the Curie-Weiss behavior of the static susceptibility.[7]

Although the theory also explained successfully other properties including the muon relaxation time above T_N for MnSi,[10] no direct observation has ever been made of the MK fluctuations by neutron scattering. The study of the energy spectra of the fluctuations is quite important for a crucial examination of the theory because the theory predicts dynamical properties which are somewhat different from those for the localized spin system as discussed in Sec. II.

It is also noted that the spin fluctuations in the paramagnetic phase of MnSi detected by the μSR (muon spin relaxation) experiment[10] resemble those of ferromagnetic materials even down to the close vicinity of the Néel temperature T_N where the helimagnetic order is established. The spin correlations in MnSi were anticipated to vary with temperature in a complicated way near T_N; another broad peak is observed one degree above T_N in the specific-heat,[11] thermal expansion coefficient[12] as well as the attenuation coefficient of the longitudinal ultrasonic wave.[13] Therefore, the temperature evolution of the spin correlations around T_N is an interesting problem for study by neutron scattering.

This paper is concerned with the observation of the MK fluctuations above T_N. In the next section, we will discuss the SCR theory to show how the fluctuations predicted by the theory can be detected by neutron scattering.[14] After giving a brief description of the experimental procedure including the method for correction of the experimental data, the experimental results are described in Sec. IV. A preliminary experimental result concerning the variation of the spin correlations with temperature from the helimagnetic phase to the paramagnetic phase is presented in Sec. IV A to show that the paramagnetic phase can effectively be treated as that of a ferromagnetic material. The results are discussed in Sec. V.

II. THE SCR THEORY AND NEUTRON SCATTERING

The neutron magnetic scattering cross section is proportional to the imaginary part of the dynamical susceptibility $\mathcal{X}(Q,\omega)$ (Ref. 15);

$$\frac{d^2\sigma}{d\Omega\,d\omega} = A\,(k_i k_f)\,|f(Q)|^2\Sigma^{\alpha\beta}(\delta_{\alpha\beta}-\hat{e}_q^\alpha\hat{e}_q^\beta)$$

$$\times S^{\alpha\beta}(Q,\omega)\,, \tag{1}$$

$$S^{\alpha\beta}(Q,\omega) = \frac{\hbar}{\pi}\,\frac{1}{1-\exp(-\hbar\omega/kT)}\,\mathrm{Im}\mathcal{X}^{\alpha\beta}(Q,\omega)$$

with the conventional notations. $S^{\alpha\beta}(Q,\omega)$ is the scattering function. According to the SCR theory, the dynamical susceptibility $\mathcal{X}(Q,\omega)$ can be expressed as[7]

$$\mathcal{X}(Q,\omega) = \frac{\mathcal{X}_0(Q,\omega)}{1-I\mathcal{X}_0(Q,\omega)+\lambda(Q,\omega)}\,, \tag{2}$$

where $\mathcal{X}_0(Q,\omega)$ is the susceptibility of the noninteracting system, I, the intra-atomic interaction, and $\lambda(Q,\omega)$ is an additional term resulting from the mode-mode coupling of the spin fluctuations. $\lambda(Q,\omega)$ is absent in the RPA theory. Since $\lambda(Q,\omega)$ contains $\mathcal{X}(Q,\omega)$, it is almost impossible to solve for $\mathcal{X}(Q,\omega)$ rigorously from Eq. (2). In the case of a weak itinerant ferromagnet where only the long-wave and low-energy fluctuations become important, $\mathcal{X}_0(Q,\omega)$ can be expanded as a series in ω and q (the deviation of Q from the reciprocal-lattice point τ) as

$$\mathcal{X}_0(Q,\omega) = \mathcal{X}_0(0,0)\left[1-Aq^2-B\left[\frac{\omega}{q}\right]^2+iC\left[\frac{\omega}{q}\right]\right]$$

$$\tag{3}$$

and $\lambda(Q,\omega)$ can be approximated by

$$\lambda(Q,\omega) = \lambda(0,0)\,. \tag{4}$$

Therefore, $\mathrm{Im}\mathcal{X}(Q,\omega)$ is reduced to

$$\mathrm{Im}\mathcal{X}(Q,\omega) = \frac{\mathcal{X}_0(0,0)C\left[\dfrac{\omega}{q}\right]}{[1+\lambda(0,0)-I\mathcal{X}_0(0,0)(1-Aq^2+\cdots)]^2+I^2C^2\left[\dfrac{\omega}{q}\right]^2}\,. \tag{5}$$

Since the static susceptibility given by

$$\mathcal{X}(0,0) = \frac{\mathcal{X}_0(0,0)}{1+\lambda(0,0)-I\mathcal{X}_0(0,0)} \tag{6}$$

obeys the Curie-Weiss law, $1+\lambda(0,0)-I\mathcal{X}_0(0,0)$

should be written as

$$1+\lambda(0,0)-I\mathcal{X}_0(0,0) = \kappa^2(T)$$

$$= \kappa_0^2(T-T_c)\,. \tag{7}$$

The scattering function $S(Q,\omega)$ of the MK fluctuations is then reduced to

$$S(Q,\omega)= \frac{\hbar}{\pi} \frac{1}{1-\exp(-\hbar\omega/kT)}$$
$$\times \frac{C''\omega q}{q^2[\kappa(T)^2+A'q^2]^2 C'^2\omega^2} \qquad (8)$$

with A', C', and C'' the appropriate constants. On the other hand, the scattering function of the critical scattering from the Heisenberg system is given by[15]

$$S(Q,\omega)= \frac{1}{\pi} \frac{\hbar\omega}{1-\exp(-\hbar\omega/kT)} \frac{C_0}{\kappa(T)^2+q^2}$$
$$\times \frac{\Gamma(q)}{\Gamma(q)^2+\omega^2} \qquad (9)$$

with

$$\Gamma(q)= \frac{Cq^2}{\chi(q)} = \frac{C(\kappa^2+q^2)q^2}{\chi_0} , \qquad (10)$$

which is reduced to

$$S(Q,\omega)= \frac{\hbar}{\pi} \frac{1}{1-\exp(-\hbar\omega/kT)}$$
$$\times \frac{C''\omega q^2}{C'[\kappa(T)^2+q^2]^2 q^4+\omega^2} . \qquad (11)$$

If we compare (11) with (8), the scattering function of the MK fluctuations can also be expressed by $\Gamma(q)$, but with $\Gamma(q)$ given by

$$\Gamma(q)=C[\kappa(T)^2+q^2]q/\chi_0 . \qquad (12)$$

Therefore, the MK fluctuations resemble the spin fluctuations of the Heisenberg system in the critical regions, but the energy spectrum has a different q dependence from that in the Heisenberg system, and this may be distinguished by neutron scattering.

III. EXPERIMENTAL PROCEDURE

The crystal used in this experiment is the same that was employed in two previous neutron scattering experiments.[2,16] It was grown by the Czochralski method and is a cylinder 20 mm in diameter and 40 mm long with [01$\bar{1}$] nearly parallel to the cylindrical axis.

The experiment was carried out on a triple-axis neutron spectrometer at the Brookhaven High Flux Beam Reactor. A pyrolytic graphite (002) mono-

chromator and analyzer were used. Most of the data were taken with the scattered neutron energy (E_f) fixed at 14.8 meV and with four horizontal collimators set either at 40'-20'-20'-40' (low resolution) or at 20'-20'-20'-20' (high resolution). Some additional data were taken with the incoming energy (E_i) fixed at 13.7 meV. A graphite filter was inserted in an appropriate beam path position to remove higher-order contamination.

The crystal was mounted with [01$\bar{1}$] vertical in a variable-temperature cryostat and most of the data were taken with constant Q mode of operation along [011] in the vicinity of the 011 reciprocal lattice point. This was the direction where the scattering was least contaminated by the Bragg tail. The measured intensity $I(Q,\omega)$ is given by the convolution of the cross section given in Eq. (1) with a resolution function of the spectrometer $R(\Delta Q,\Delta\omega)$ given originally by Cooper and Nathans[17]

$$I(Q,\omega)= \int \frac{d^2\sigma}{d\omega\,d\Omega}(Q',\omega')$$
$$\times R(Q-Q',\omega-\omega')d\omega'dQ' . \qquad (13)$$

Good agreement between the observed spectra and the calculated spectra is obtained for the phonon scattering as shown in I. The instrumental resolution is approximately 0.45 meV full width at half maximum (FWHM) for high-resolution measurements and is 0.65 meV for low-resolution measurements as later seen in Fig. 5.

In order to combine $\chi(q)$ obtained by low-resolution measurements with that by high-resolution ones, the scattering intensity was normalized at a wave vector of $\zeta=0.1$ by overlapping the data of both resolutions at this point.

IV. EXPERIMENTAL RESULTS

A. Spin correlations near T_N

In order to see how the satellite Bragg reflection develops into the critical scattering, two-dimensional mapping of the magnetic scattering was carried out in the (01$\bar{1}$) reciprocal-lattice plane using cold neutrons with $E_i=5$ meV and with the energy transfer $\hbar\omega=0$. The results at three different temperatures are displayed in Fig. 1, where solid lines in the figure are the contour lines of equal intensity of scattering. At 28.5 K, just below the Néel temperature of 29 K, a Bragg reflection

MnSi (ξ,ζ,ζ)

$\xi \times 10^{-3}$

$E_0 = 5$ meV
CL 20-10-10-20
28.5 K
(a)

[100]

29 K
(b)

30 K
(c)

$\zeta \longrightarrow$ [011]
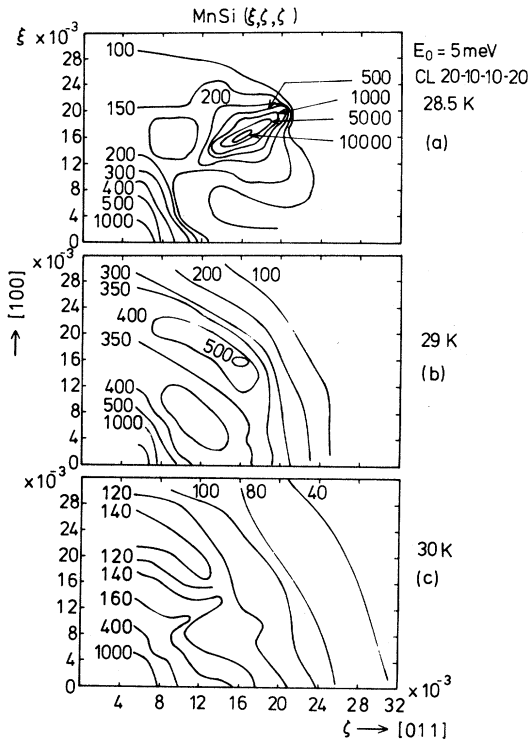
FIG. 1. Contour maps of equal intensity of critical scattering around a satellite point measured with $E_i = 5$ meV with $\hbar\omega = 0$ at three different temperatures.

was detected at $\vec{Q} = (\zeta,\zeta,\zeta)2\pi/a$ with $\zeta = 0.016 \pm 0.001$ ($Q = 0.038 \pm 0.002$ Å^{-1}), which is nearly in agreement with the previous measurement of $Q = 0.035$ Å^{-1} at 4.2 K by the small-angle scattering machine of the Institut Laue Langevin (ILL) ($D11$). When the temperature increases by 0.5°, the satellite peak starts to elongate in the direction perpendicular to the Q vector as shown in Fig. 1(b) and the critical scattering finally develops around the (0,0,0) center as a circular ring with $Q = 0.038$ Å^{-1}, in sharp contrast with the conventional case where the critical scattering develops around the satellites. With a further increase of temperature by one degree, the ring practically disappears and the intensity of scattering simply tends to increase with decreasing wave vector; the spin correlations resemble those of simple ferromagnets. Therefore, the spin fluctuations above 30 K can be treated as those of a simple ferromagnet, especially for wave vectors greater than $\zeta = 0.03$.

Temperature variations of the peak intensities of the elastic scattering ($\hbar\omega = 0$) measured at two different points in reciprocal lattice space $\vec{Q}_1 = (0.01,0.01,0.01)2\pi/a$ and

$\vec{Q}_2 = (0,0.95,0.95)2\pi/a$ are shown in Fig. 2. Figure 2(a) is the result of the high-resolution measurement ($E_i = 5$ meV), and it represents the temperature evolution of the spin correlations corresponding to the helical spin order, while the results shown in Fig. 2(b) were obtained by low-resolution measurements ($E_i = 14.7$ meV). The result of the high-resolution measurement is also plotted in (b) by a broken line for comparison. Note that there is almost no anomaly in the spin correlations at the $\vec{Q}_2$ position at T_N. The results in Figs. 1 and 2 suggest that the spin correlations corresponding to the helical spin order become significant only in the close vicinity of the Néel temperature and they are condensed into the narrow wave-vector region around the Q vector of the helical spin order. The overall behavior of the spin correlations would be that of the ferromagnetic order and it seems to be divergent at a temperature slightly different from T_N. The critical scattering from MnSi was measured first with $D11$ (ILL) and similar results had been obtained.[18]

MnSi
(a)

$E_0 = 5$ meV
CL 20-10-10-20
(0.01,0.01,0.01)

Neutron Counts

28   29   30 (K)

$E_F = 13.7$ meV   (b)
CL 20-40-40-40
(0,0.95,0.95)

Neutron Counts

10   20   30 (K)
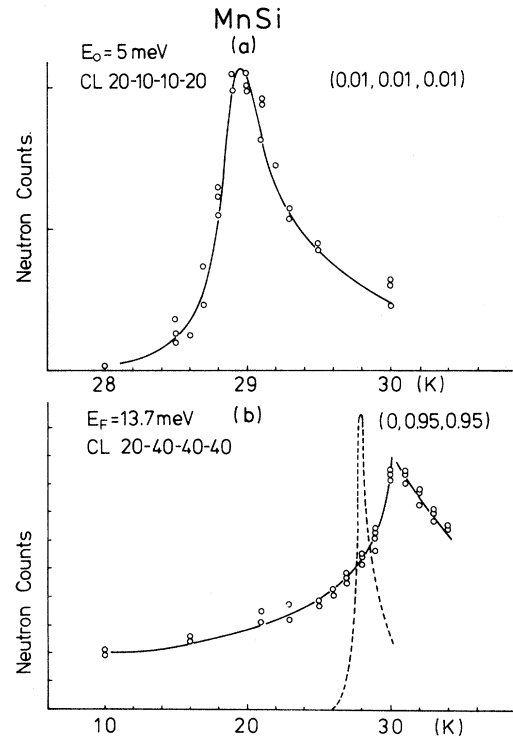
FIG. 2. Temperature variation of peak intensities at two different Q positions (a) $\vec{Q}_1 = (0.01,0.01,0.01)2\pi/a$ and (b) $\vec{Q}_2 = (0,0.95,0.95)2\pi/a$. The former was measured with $E_i = 5$ meV, while the latter with $E_i = 14.7$ meV.

B. Measurements of MK fluctuations

Since the MK fluctuations appear around $\hbar\omega=0$ as the low-energy excitations above T_N, the most important task was to accurately subtract the background due to the nuclear incoherent scattering. We could not estimate it from the high-temperature scattering, because an appreciable amount of the magnetic scattering was still detected even at room temperature. Since the intensity of the incoherent scattering, in principle, varied with temperature and with wave vector, we could not estimate the background from the scattering with high momentum transfers measured at high temperatures. Fortunately we found that the scattering at $\vec{Q}=(0,0.6,0.6)2\pi/a\,(\zeta=0.4)$ was practically free of any contribution from magnetic scattering as shown in Fig. 3(a). The intensity as well as the width of the scattering did not depend on temperature over a wide range of temperature through T_N within the experimental errors. The profile of scattering also agreed reasonably with that calculated by Eq. (13) as indicated by a broken line in the figure. The wave-vector dependence of the background was also found to be small as seen in Fig. 3(b) where the scattering profiles measured
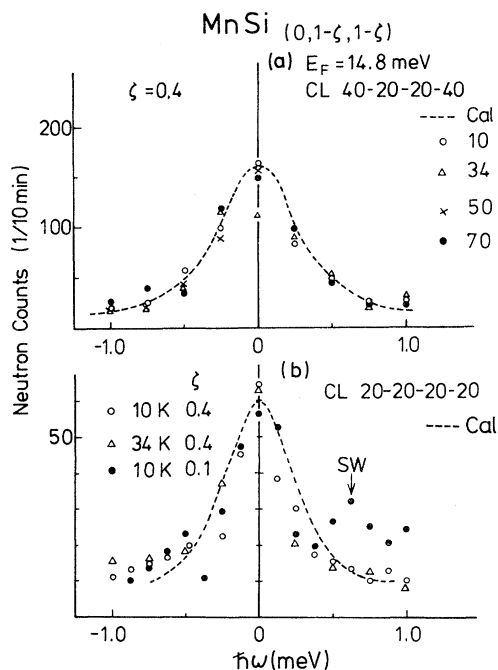
at 10 K for two different wave vectors of $\zeta=0.4$ and 0.1 are displayed. Except for a small peak at $\hbar\omega=0.7$ meV for $\zeta=0.1$ probably due to the spin-wave excitations, the background scattering does not depend appreciably on the wave vector. The same conclusion was obtained by the profile calculation. Therefore, we subtracted from the observed scattering the intensity of the scattering at $\zeta=0.4$ at each temperature as the background.

In order to demonstrate the contribution of the background in the observed scattering, the profiles of the measured spectra (open circles) are compared with those of the magnetic scattering corrected for the background (closed circles) in Fig. 4. The figure indicates that the correction is only a small fraction of the observed spectra for temperatures near T_N and at small ζ values, but it becomes significant at high temperatures and the main origin of the error. The profiles of the magnetic scattering thus determined agree satisfactorily with that calculated by Eq. (13) using the cross section given by (9), which are plotted by solid lines in the figure. The parameters Γ determined are also shown in the figure.

Some examples of the paramagnetic scattering determined in this way are demonstrated in Fig. 5. The left-hand side is the variation of scattering with wave vector, while the temperature variation of the scattering at a constant $\vec{Q}$ is shown in the right-hand side. The solid lines are calculated by Eqs. (9) and (13) with the values of Γ attached to each profile. The agreement between the observation and the calculated was satisfactory and we could determine Γ with good accuracy. Note that the intensity of the scattering practically falls down to the background when the energy transfers exceed 2 meV. This means that the resolution of

FIG. 3. (a) Energy spectra of incoherent scattering (background) measured at $\vec{Q}_1=(0,0.6,0.6)2\pi/a$ at various temperatures. (b) Energy spectra of the background measured at two different wave vectors at 5 K.
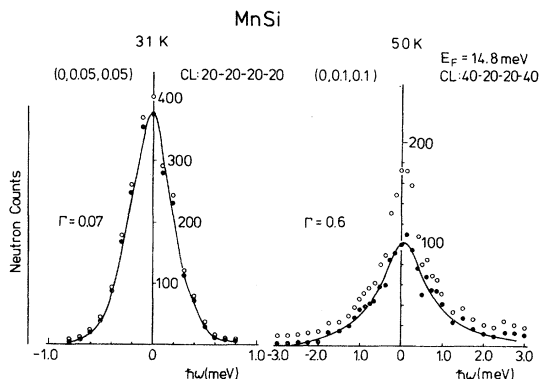
FIG. 4. Comparison of observed spectra (open circles) and that corrected for background (closed circles) measured with two different conditions.
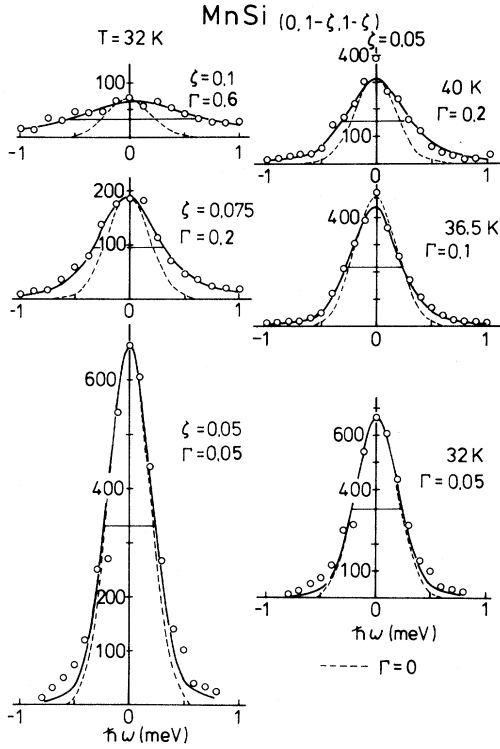
FIG. 5. Examples of variation of energy spectra of paramagnetic scattering with temperature T (right-hand side) and with wave vector ζ (left-hand side). Correction was made for background. Solid lines are calculated by Eqs. (9) and (13) with Γ attached to each profile. Broken lines correspond to the cases for $\Gamma = 0$.

the spectrometer was good enough to separate the MK fluctuations from the excitations in the Stoner continuum. Therefore, the integration of the spectra to get the generalized susceptibility could also be performed with good accuracy. If measured

with a poor resolution spectrometer, the magnetic scattering at a given wave vector could be observed up to 20 meV as reported in I.

In the actual calculation of the profile by Eqs. (13) and (9) to get Γ, the inverse correlation length $\kappa(T)$ should be known. This quantity can, in principle, be determined experimentally with a two-axis spectrometer as is usually done in most of the measurements of critical scattering. Unfortunately, this method could not be adopted in the present case because of the presence of the high-energy excitations even at high temperatures. Therefore, we determined $\kappa(T)$ by iteration; at first, a proper value was assumed for $\kappa(T)$ to evaluate Γ. Then the generalized susceptibility $X(q)$ was calculated by integrating the observed spectra and $\kappa(T)^2$ was estimated by extrapolating $X(q)$ to $q = 0$. The new value of $\kappa(T)$ was then employed to recalculate the energy spectra and $X(q)$ was determined. This process was repeated until $\kappa(T)$ and $X(q)$ converged to the final values. One example of iteration is demonstrated in Table I. The starting value of $\kappa = 0.270$ differs by 20% from the value $\kappa = 0.216$ obtained by extrapolating the calculated $1/X(q)$ to $q = 0$; $[1/X(0) = A\kappa^2(T)]$. If we use, however, the obtained value to recalculate X, κ obtained by extrapolation agrees satisfactorily with the assumed value. In Fig. 6 is shown the temperature and wave-vector dependences of the generalized susceptibility $X(q)$ thus determined, where the reciprocal of $X(q)$, $1/X(q)$ is plotted as a function of T or of q^2. Except for $X(q)$ at temperatures close to T_N where the analyzed data are scattered to some extent, a linear relation between $1/X(q)$ and T or q^2 nearly holds between 34 and 70 K and for ζ up to 0.125. Therefore, $X(q)$ can be expressed as

TABLE I. Results of iteration of analysis of spectra at 70 K.

$\kappa = 0.270$ (starting value)			$\kappa = 0.216$ (starting value)		
ζ	Γ (meV)	$1/X(Q)$	Γ	$1/X(Q)$	$\Delta(1/X)$ (%)
0.03	0.15	2.071	0.15	2.038	−1.6
0.05	0.318	2.956	0.319	2.921	−1.2
0.075	0.5	3.372	0.5	3.387	0.5
0.1	1.0	4.188	1.0	4.193	0.1
0.125	1.106	4.710	1.14	4.690	−0.4

$\zeta \rightarrow 0 \quad \dfrac{1}{X(0)} \rightarrow 2.212$

$\dfrac{1}{X(0)} \rightarrow 2.198$

κ from $\dfrac{1}{X(0)} = 0.216$

κ from $\dfrac{1}{X(0)} = 0.216$
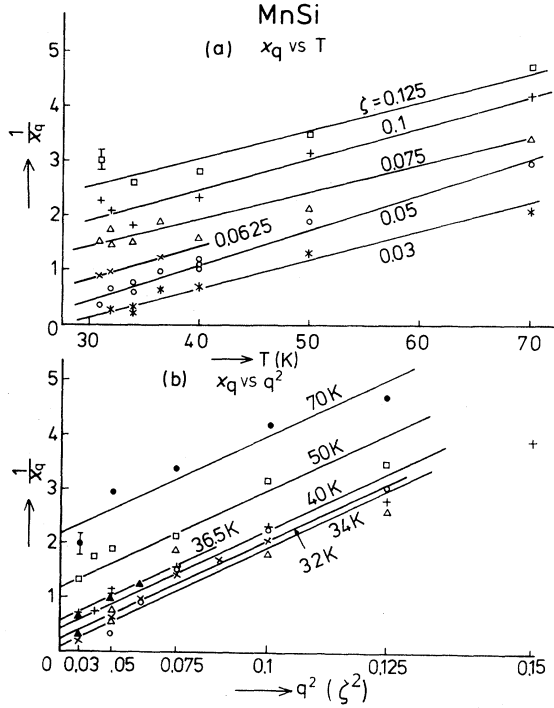
FIG. 6. (a) Temperature dependence of inverse of susceptibility, $1/X_q$ at different wave vectors ζ, (b) wave-vector dependence of $1/X_q$ at different temperatures plotted against ζ^2.

$$X(q) = \frac{C_q}{\kappa(T)^2 + q^2} , \qquad (14)$$

with $\kappa(T)^2 = \kappa_0^2(T - T_c)$ in these temperature and momentum ranges.

In order to estimate $X(0,T)$ from $X(q,T)$, two procedures were tried. One was to determine C_q in
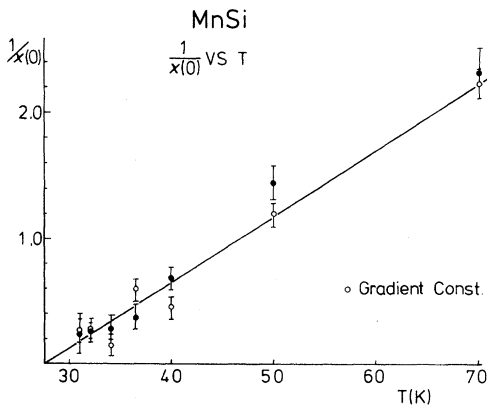
FIG. 7. Temperature variation of static susceptibility $X(0)$ estimated by extrapolation of Fig. 6(b) to $\zeta = 0$. Open circles correspond to the results obtained with an assumption that all $X(q)$ obey the Curie-Weiss law with the same Curie constant.

Eq. (14) by the least-mean-squares fitting to data at each temperature and another was to assume C_q constant for all the data studies. The values of $1/X(0)$ obtained by these two procedures are plotted as a function of T in Fig. 7. The values determined by the latter procedure are denoted as "Gradient Const." The difference between the results obtained in these two procedures is rather small. The error bars in the figure were estimated from the difference of the results obtained by measurements with different experimental conditions (resolutions). The figure shows clearly the Curie-Weiss relation

$$X(0) = \frac{C_0}{T - T_c} \qquad (15)$$

nearly holds over the studied temperature range with $T_c = 28 \pm 1$ K, suggesting that the observed fluctuations are really responsible for the Curie-Weiss relation of the static susceptibility and therefore they correspond to the MK fluctuations. A slight deviation of $1/X(0)$ from the Curie-Weiss relation below 34 K would partly be due to the complicated situation that, below this temperature, the magnetic fluctuations start to condense around the satellite points, resulting in suppressing the fluctuations in the regions far from the satellite points where the present measurements were carried out.

The linewidth Γ determined by this analysis is plotted against both $q^2(\kappa^2 + q^2)$ and $q(\kappa^2 + q^2)$ in Fig. 8, where we find that the linewidths at different temperatures and wave vectors fall on a single curve in both cases. The accuracy of determined Γ values are shown by error bars attached to some data points, which were estimated from the data obtained by the measurements with different resolution. For Γ less than 0.5, the error for fitting a single spectrum is about ± 0.03 meV. The results provide us with an experimental evidence that Γ is inversely proportional to $X(q)$ as is anticipated theoretically. Furthermore, a linear relation is achieved for the $(\kappa^2 + q^2)q$ plot in the low-q range. Therefore, the MK fluctuation model was found to be more appropriate than the Heisenberg model.

V. DISCUSSION

A. Spin correlation near T_N

Temperature evolution of spin correlations in the close vicinity of T_N is quite unique. We found that the critical scattering developed not around
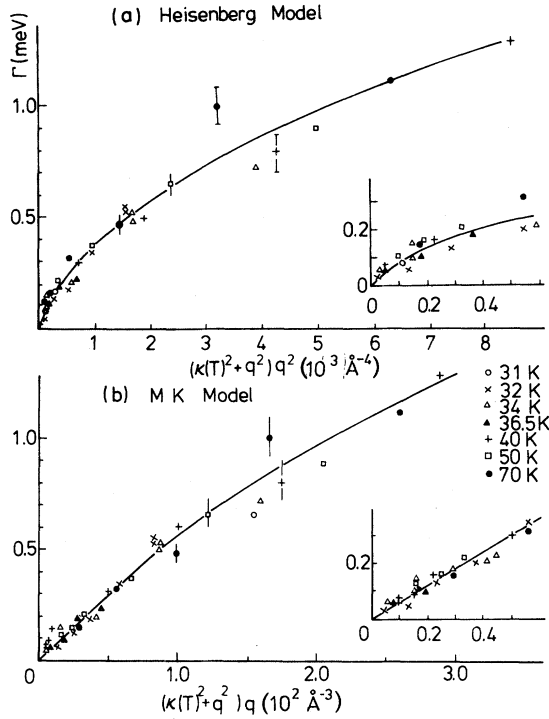
FIG. 8. Linewidth Γ of spin fluctuations plotted against $q^2[\kappa(T)^2+q^2]$ (a) and $q[\kappa(T)^2+q^2]$ (b). Insets to the figure are plots in enlarged scales around zero point. Solid lines are only a guide for the eyes.

the satellite points but around (0,0,0) as a ring with a radius q corresponding to the wave vector of the helical order. With a slight increase of temperature by one degree, the ring apparently disappeared and diffuse scattering centered at (0,0,0) developed just as is the case with the critical scattering of the ferromagnet. Note that a similar temperature variation of the critical scattering has been observed in Cr,[19] a typical itinerant antiferromagnet, where the diffuse scattering develops not around $(0,0,1\pm\delta)$, but around (0,0,1) above $T/T_N=1.1$. Although the peculiar temperature variation of the critical scattering in MnSi can be anticipated in general for the helical spin system with small energy difference from the ferromagnetic structure, a similarity between MnSi and Cr evokes a conjecture that the behaviors would be related with an important characteristic of the itinerant electron system where the spin fluctuations are condensed in a narrow wave-vector region in reciprocal space[8,9] as will be discussed in more detail below.

The spin fluctuations in MnSi near T_N have been discussed by Makoshi based on the SCR theory,[20] and detailed studies of the critical scatter-

ing using the small-angle scattering machine at KENS (KENS-SAN) are also in progress. Therefore, a crucial comparison between the theory and experimental results will be made separately.

B. MK fluctuations

The magnetic excitations detected by neutron scattering in MnSi above T_N have the characteristics of the weak itinerant ferromagnet predicted by the MK SCR theory. In addition to the broad magnetic excitations in the Stoner continuum which were observed above 4 meV up to 300 K without significant temperature change, the low-energy excitations could be detected below 2 meV. The excitations have a linewidth Γ which varies with temperature and wave vector as the MK theory predicted for the weak itinerant ferromagnet. Furthermore, the temperature and wave-vector dependences of $X(q)$ could be determined and we found that $X(0)$ obtained by extrapolating $X(q)$ to $q=0$ obeys the Curie-Weiss law. Therefore, we may conclude that the observed excitations correspond to the MK fluctuations in the weak itinerant ferromagnet.

Another important characteristic of $X(q)$ in the weak itinerant ferromagnet predicted by the SCR theory is that $X(q)$ should vary strongly with wave vector; the generalized susceptibility should obey the Curie-Weiss law only in a limited range of q, in contrast with the Heisenberg model where the Curie-Weiss law holds for all the q values with the same Curie constant. In the unified SCR theory,[9] Moriya and co-workers developed the method to calculate the dynamical susceptibility for the system with a local moment S_L^2 on the atom, $X(q,\omega,S_L^2)$. Since S_L^2 is related with the dynamical susceptibility by the fluctuation-dissipation theorem as

$$
\begin{aligned}
S_L^2 &= \frac{1}{N}\sum_j \langle S_j^2 \rangle = \frac{1}{N^2}\sum_q \langle S_q S_{-q} \rangle \\
&= \frac{3kT}{N^2}\sum_q X(q,S_L^2) \\
&= \frac{3kT}{N^2}\sum_q \int \frac{\mathrm{Im}X(q,\omega,S_L^2)}{\omega}d\omega ,
\end{aligned}
\tag{16}
$$

S_L^2 can be determined from Eq. (16) in a self-consistent way. By this process, they have found that $\sum_q X(q)$ is almost temperature independent in the weak itinerant ferromagnet and have concluded

that the amplitude of the local moment S_ζ^2 in this system increases, rather than decreases, with temperature [see Eq. (16)]. The Curie-Weiss relation is the result of the increase of this amplitude. Actually we have found that the magnetic part of the thermal expansion coefficient becomes positive just above T_N,[12] suggesting the increase of S_ζ^2 with temperature above T_N as predicted by the theory. Therefore, the direct observation of the q dependence of $X(q)$ would provide the crucial examination to the SCR theory.

We have shown in Fig. 6 that $X(q)$ obeys Eq. (14) with C_q constant over the wide range of temperature and for $\zeta \le 0.125$. These behaviors closely resemble those found in the Heisenberg system. However, if we compare carefully the T dependence [Fig. 6(a)] and the q^2 dependence [Fig. 6(b)] of $1/X(q)$, we find that the q dependence is unusually strong in MnSi. In the molecular-field approximation, the generalized susceptibility $X(q)$ of the Heisenberg system is given by

$$X(q) = \frac{\chi_c}{(T/T_c - 1) + [1 - J(q)/J(0)]} , \quad (17)$$

where $\chi_c = Ng^2\mu_B^2 S(S+1)/3kT_c$ and $J(q)$ is the Fourier transform of the exchange parameter J_r. Equation (14) follows by expanding $J(q)$ in a series of q.

In the simplest case of a simple cubic ferromagnet with only the nearest-neighbor interaction J, $[J(0)-J(q)]/J(0)$ at $(0,\zeta,\zeta)$ being

$$[J(0)-J(q)]/J(0) = (\tfrac{4}{3})\sin^2\pi\zeta , \quad (18)$$

it takes the maximum value of $\tfrac{4}{3}$ even at the zone boundary of $\zeta = 0.5$. Therefore, a relation

$$1/X_q(\zeta=0, 2T_c) = 0.75 \; 1/X_q(\zeta=0.5, T_c) \quad (19)$$

holds in this material. In Fig. 9, the $1/X(0)$ vs T and $1/X_q(T_c)$ vs q^2 plots are compared in a normalized abscissa scale of $(T-T_c)/T_c$ and $[J(0)-J(q)]/J(0)$. In the Heisenberg system, both plots fall on a single solid line. In the figure is also plotted $1/X_q(\zeta, T_c)$ of MnSi against ζ which was calculated from $[J(0)-J(q)]/J(0)$ by Eq. (18). The figure shows clearly that the decrease of $X(q)$ with increasing q is quite significant for MnSi compared with the Heisenberg system. The result means that the effective magnetic interactions between the local moments in MnSi are much larger than the values expected from T_c. This fact is
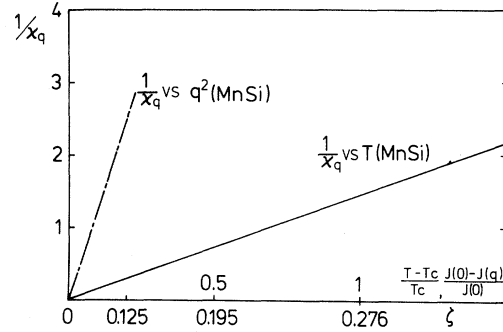
FIG. 9. $1/X(0)$ vs T and $1/X_q(T_c)$ vs q^2 relations plotted against $(T-T_c)/T_c$ and $[J(0)-J(q)]/J(0)$, respectively. In the Heisenberg system both relations fall on a single solid line. In MnSi, the $1/X_q$ vs q^2 plot was made against ζ calculated using Eq. (18) in the text from $[J(0)-J(q)]/J(0)$ in the abscissa.

consistent with our finding that the observed spin-wave excitations explain only a fraction of the decrease of the magnetization for MnSi[12,21]; the Curie temperature of the material is determined not by the magnetic interactions, but by other mechanisms, such as those giving rise to the Stoner excitations. Therefore, the spin correlations can remain significant even at very high temperatures of order $T/T_N = 2.5$, just as is the case with the low-dimensional materials.

In order to continue discussions of the q dependence of $X(q)$, it is important to extend the measurement to the zone boundary. However, we found it quite difficult to perform because of the steep decrease of $X(q)$ with q and steep increase of Γ with q. If we extrapolate, for example, $X(q)$ and Γ to $\zeta = 0.4$ by assuming that the relations found for lower q values also hold up to $\zeta = 0.4$, the peak value of the energy spectra of the magnetic scattering becomes very small, of order 2% of the nuclear incoherent scattering even at 34 K, which is really within the experimental errors.

Finally, it is remarked that the atomic moment on Mn atoms in MnSi should be determined following Eq. (16); $X(q)$ can be determined by integrating the intensity of the magnetic inelastic scattering at q over the wide energy range exceeding 20 meV, while S_ζ^2 can be obtained by integrating $X(q)$ over the whole Brillouin zone. The conventional method of determining the moment by means of paramagnetic scattering from the powder sample as was done by Ziebeck and Brown[6] give a meaningless result because it neglects a priori the q

dependence of $\chi(q)$, which is not correct for the material.

In conclusion, we could successfully separate the low-energy magnetic fluctuations from the excitations in the Stoner continuum in MnSi above T_N and the generalized susceptibility $\chi(q)$ corresponding to the fluctuations could be determined by integrating the energy spectra over the energy, which was found to vary with temperature and q following Eq. (14) with a constant C_p. $\chi(0)$ obeys the Curie-Weiss law, but the q dependence of $\chi(q)$ is quite significant compared with the conventional Heisenberg system. Furthermore the linewidth Γ varies with temperature and q following the relation $\Gamma \propto q/\chi(q,T)$ in contrast with $\Gamma \propto q^2/\chi(q,T)$ predicted for the Heisenberg system. All these features are consistent with what the SCR theory predicted and thus we provide the first direct experimental evidence of the presence of the MK fluctuations in the weak itinerant ferromagnet. We hope that our experimental results stimulate further theoretical study of this material as the calculation of $\chi(q)$ based on the realistic band model, so as to make possible a quantitative comparison of the experimental results with the theory.

[1]Y. Ishikawa, K. Tajima, D. Bloch, and M. Roth, Solid State Commun. 19, 525 (1976).

[2]D. Bloch, J. Voiron, V. Jaccarino, and J. H. Wernick, Phys. Lett. 51A, 259 (1975).

[3]Y. Ishikawa, G. Shirane, and J. A. Tarvin, Phys. Rev. B 16, 4956 (1977).

[4]L. M. Levinson, G. H. Lander, and M. O. Steinitz, in *Magnetism and Magnetic Materials—1972 (Denver),* Proceedings of the 18th Annual Conference on Magnetism and Magnetic Materials, edited by C. D. Graham and J. J. Rhyne (American Institute of Physics, New York, 1973), p. 1138.

[5]H. Yasuoka, V. Jaccarino, R. C. Sherwood, and J. H. Wernick, J. Phys. Soc. Jpn. 44, 842 (1978).

[6]K. R. A. Ziebeck and P. J. Brown, J. Phys. F 10, 2015 (1980).

[7]T. Moriya and A. Kawabata, J. Phys. Soc. Jpn. 34, 639 (1973); 35, 669 (1973).

[8]T. Moriya, J. Magn. Magn. Mater. 14, 1 (1979).

[9]T. Moriya, in *Proceedings of the Taniguchi International Symposium on Electron Correlation and Magnetism in Narrow Band System,* edited by T. Moriya (Springer, Berlin, 1981), p. 2.

[10]R. S. Hayano, H. J. Uemura, J. Imazato, N. Nishida, T. Yamazaki, H. Yasuoka, and Y. Ishikawa, Phys. Rev. Lett. 41, 1743 (1978).

[11]A. Ikeda, Master thesis, Tohoku University, 1978 (unpublished).

[12]M. Matsunaga, Master thesis, Tohoku University, 1980 (unpublished); M. Matsunaga, Y. Ishikawa, and T. Nakajima, J. Phys. Soc. Jpn. (in press).

[13]S. Kusaka, K. Yamamoto, T. Komatsubara, and Y. Ishikawa, Solid State Commun. 20, 927 (1976).

[14]Y. Ishikawa, J. Magn. Magn. Mater. 14, 123 (1979).

[15]W. Marshall and S. W. Lovesey, *Theory of Thermal Neutron Scattering* (Oxford University, New York, 1971), p. 241.

[16]J. A. Tarvin, G. Shirane, Y. Endoh, and Y. Ishikawa, Phys. Rev. B 18, 4815 (1978).

[17]M. J. Cooper and R. Nathans, Acta Crystallogr. 28, 357 (1968).

[18]M. Roth and Y. Ishikawa (unpublished).

[19]C. R. Fincher, Jr., G. Shirane, and S. A. Werner (unpublished).

[20]K. Makoski, J. Phys. Soc. Jpn. 46, 1767 (1979).

[21]Y. Ishikawa, in *Physics of Transition Metals, 1980,* edited by P. Rhodes (Institute of Physics, London, 1981), p. 357.